Laser isotope separation of 176Lu through off-the-shelf lasers

Mv Suryanarayana (suryabarcv@gmail.com)
Bhabha Atomic Research Centre
Manda Sankari
Bhabha Atomic Research Centre

Research Article

Keywords: laser isotope separation, 176Lu isotope, lasers, atomic systems

Posted Date: March 19th, 2021

DOI: https://doi.org/10.21203/rs.3.rs-296419/v2

Laser isotope separation of ^{176}Lu through off-the-shelf lasers

MV Suryanarayana* and M Sankari
Laser & Plasma Technology Division
Bhabha Atomic Research Centre
Visakhapatnam 530 011, Andhra Pradesh, India
*** Corresponding author email: suryam@barc.gov.in**

Abstract

We propose a novel and simple method for the laser isotope separation of ^{176}Lu a precursor for the production of ^{177}Lu medical isotope. The physics of the laser-atom interaction has been studied through the dynamics of the atomic level populations using the density matrix formalism. It has been shown that a combination of cw excitation lasers and pulsed ionization laser can be used for the laser isotope separation of ^{176}Lu. The optimum conditions for the efficient and selective separation of ^{176}Lu have been derived by studying the time evolution of level population under laser excitation. It has also been shown that, it is possible to produce ~100% enriched ^{176}Lu isotope at a rate of 5 mg / hour, which is higher than all previously reported methods so far. The isotope separation process proposed can be easily adopted using off-the-shelf lasers, for similar atomic systems.

Introduction

Atomic Vapor Laser Isotope Separation (AVLIS) of actinides (particularly Uranium) has applications in nuclear industry and defence[1]; therefore, a lot of research has been carried out to achieve the above objective. The technology thus developed is largely limited to a handful technologically advanced nations and strongly controlled due to proliferation risks. Most of the AVLIS activity is centred on utilization of high repetition rate Copper Vapor Laser (CVL) or Solid-State Laser (SSL) pumped dye laser systems for the excitation and ionization of the desired isotope(s). The high pulse repetition frequency (PRF) (10 KHz or higher) of these lasers ensures high interaction efficiency with the atomic vapor enabling the production of the desired isotopes in large scales. It has been realised that AVLIS technology has the ability to play a pivotal role in nuclear medicine[2].

^{177}Lu isotope has gained importance in the targeted radionuclide therapy of small tumors and metastatic lesions[3,4]. ^{177}Lu can be produced in a nuclear reactor by irradiation of its precursor (or parent) ^{176}Lu isotope. The cross-section of the nuclear reaction is 2090 b. ^{177}Lu having a half-life of 6.65 d decays to ^{177}Hf emitting β–particles with energies 497 keV (76%), 384 keV (9.7%) and 176 keV (12%). The ^{177}Hf which is formed in nuclear excited states decays to the ground state emitting low energy γ–radiation with energies 208 keV (11%) and 113 keV (6.6%). With mean penetration depths of β–particles in sub-mm, the radionuclide ^{177}Lu is capable of delivering energy in small volumes, thus having localized cytotoxic effect on the disease cells. The γ–radiation is useful for imaging; studies of bio-distribution and excretion kinetics of the infused radionuclide. Due to these advantages, ^{177}Lu has evolved as the most effective theranostic (therapeutic + diagnostic) isotope in nuclear medicine. However, natural Lu cannot be used for the production of ^{177}Lu due to the low natural abundance of its precursor isotope ^{176}Lu (2.59%). It is required to be enriched to ≥ 50% level[5]. The typical administered quantity[4] of ^{177}Lu per course for a patient is ~ 7.4 GBq (1.8 μg). Therefore, after taking into account the conversion efficiency, one milligram of enriched ^{176}Lu can be used for the treatment of > 60,000 patients after irradiation. Despite the requirements in small quantities, currently only a very few laboratories in the world have the ability to produce enriched ^{176}Lu isotope leading to the worldwide shortage of this isotope. This is primarily due to the non-availability of the suitable commercial tunable narrow band high repetition rate lasers.

AVLIS exploits the small resonance frequency shifts between the constituent isotopes of an element (called isotope shifts). The lasers in the step-wise ionization are resonantly tuned to the desired isotope causing preferential ionization enabling the separation from the rest of the isotopes. However, laser isotope separation of Lutetium is extremely complex. Unlike Uranium, the nuclear volume changes[6] in adjacent isotopes of stable Lu isotope are small (0.041 fm^2) resulting in small field shift. Therefore, the isotope shift of the transitions, which consists of field and mass shifts, are now determined only by the mass shifts. Since the mass shift is also small for the adjacent isotopes of mid and high-z elements, the overall isotope shift is small. Fortunately, in case of Lutetium, both

stable isotopes of Lu (^{175}Lu and ^{176}Lu) have widely varying nuclear spin, magnetic moment and quadrupole moment values. Consequently, ^{176}Lu has a widely spread hyperfine spectrum than the interfering ^{175}Lu isotope, which can be exploited for the enrichment of ^{176}Lu.

Kurchatov Institute[7], Moscow has reported successful enrichment of ^{176}Lu to > 68 % with production rate of ~ 4 mg / hour. They have used the following photoionization scheme for the enrichment of ^{176}Lu.

$$5d6s^2\ {}^2D_{3/2}\ (0.0\ cm^{-1}) \xrightarrow{540.4068\ nm} 5d6s6p\ {}^4F^o_{5/2}(18504.58\ cm^{-1}) \xrightarrow{535.0626\ nm}$$

$$5d6s7s\ {}^4D_{3/2}(37193.98\ cm^{-1}) \xrightarrow{618.0061\ nm} 53375\ cm^{-1} Autoionization\ State \rightarrow Lu^+$$

We have recently studied[8] the isotope selective photoionization of ^{176}Lu and optimization of the process conditions for the enrichment of ^{176}Lu through the above photoionization scheme using density matrix formalism. The obtained results were in good agreement with the reported experimental data[7]. Further, we have recently reported a new possible photoionization pathway for the enrichment of ^{176}Lu using broad band dye lasers[9]. However, most of these schemes are accessible by high repetition rate (10 – 30 kHz) CVL or SSL pumped dye laser systems. Since these laser systems have global restrictions, isotope separation using the above scheme(s) cannot be easily adopted by all the producers of nuclear medicine. This is severely restricting the availability of enriched ^{176}Lu isotope resulting in global shortage of the ^{177}Lu medical isotope.

In order to enhance the production of enriched ^{176}Lu isotope, it is required to look into the photoionization schemes which are easily accessible by off-the-shelf lasers. In the present work, we have theoretically studied the possibility of using off-the-shelf lasers for the enrichment of ^{176}Lu isotope.

Photoionization of Lu

Lutetium has two stable isotopes. They are ^{175}Lu (97.41%) and ^{176}Lu (2.59%). It has a ground state configuration of $5d6s^2\ {}^2D_{3/2}$ (0 cm^{-1}) and has an ionization potential of 43762.60 cm^{-1}. From the known energy levels[10] of Lu, it is possible to formulate innumerable multi-step photoionization schemes. Apart from the well-known first excitation transitions 540.4068 nm and 573.8130 nm

accessible by dye lasers, several strong first excitation transitions[11] exist between the wavelength range 272 nm – 495 nm. Among them, the transitions between the wavelength range of 350 nm – 495 nm are accessible by continuous wave (cw) diode laser or second harmonic of the Ti:Sapphire lasers. The hyperfine structure[13] of Lu isotopes of several photoionization schemes originating from these transitions have been studied for the relative separation of the hyperfine components of the constituent isotopes. A list of possible photoionization schemes which showed good separation of the most intense hyperfine component of ^{176}Lu from the hyperfine structure of ^{175}Lu have been tabulated in Table 1. The requisite wavelengths for these schemes are accessible by commercially available diode lasers or Ti:Sapphire lasers (fundamental frequency or through second harmonic generation). Among them, the following excitation transition has been considered for further discussion.

465 nm – 1179 nm Scheme

$$5d6s^2\ {}^2D_{\frac{3}{2}}\ (0.0\ cm^{-1}) \xrightarrow{465.9316\ nm} 5d6s6p\ {}^2D^o_{\frac{5}{2}}(21462.38\ cm^{-1}) \xrightarrow{1179.8686\ nm}$$

$$5d^26s\ {}^2P_{\frac{3}{2}}\ (29937.9\ cm^{-1}) \rightarrow Autoionization\ State \rightarrow Lu^+$$

Photoionization of Lu through pulsed blue dye lasers[14] for the first step excitation transition was reported way back in 1981. Later, photoionization schemes originating from UV-blue wavelength region[15-16] have been studied for the photoionization of Lu using second and third harmonics of the pulsed Ti:Sapphire lasers to access the requisite wavelengths. However such lasers have linewidths in several GHz, hence, cannot be easily adopted for the isotope separation of Lu.

Utilization of diode lasers for isotope separation was first reported by Olivares[17] et al, wherein two-step photoionization method was used for the isotope separation of Li isotopes. Recently Matsuoka[18] et al have studied isotope separation of ^{48}Ca using diode lasers. In both cases ionization has been carried out by a non-resonance ionization process using pulsed lasers. Further, applicability of such a method for large scale separations has not been stated.

The isotope shifts for the first and second excitation transitions of Lu are typically in the range of 400 MHz and 100 MHz respectively. From the hyperfine structure constant data[12,13] (Table 2), the frequency positions of the two-step hyperfine excitation pathways have been calculated and tabulated in Table 3. As it can be seen from the Table 3, the most intense hyperfine excitation pathway 17/2-19/2-17/2 at the frequency position (15148.7 MHz, -25159.4 MHz) of ^{176}Lu is well separated from the nearest and the most intense hyperfine excitation pathway 5-6-5 which is at the frequency position (11099.0 MHz, -17718.8 MHz) of ^{175}Lu.

The schematic of the photoionization scheme is shown in Fig. 1. The atoms in the ground state $5d6s^2$ $^2D_{3/2}$ (0.0 cm^{-1}) are excited to the 5d6s6p $^2D^0_{5/2}$ (21462.38 cm^{-1}) level using the 465.9316 nm laser and atoms from this level are further excited to the $5d^26s$ $^2P_{3/2}$ (29937.9 cm^{-1}) level using the 1179.8686 nm laser, which are eventually ionized using an ionization laser through either auto-ionization level or non-resonant ionization. During the excitation process, due to the finite life-time of the resonant states, the atoms decay either back to their original states or into the trapped states and lost from ionization process. The excitation rates, decay[11] rates of atoms and the ionization rates are also given in Fig. 1.

In a laser isotope separation process, the atomic parameters such as isotope shifts, hyperfine structures of the constituent isotopes, radiative lifetimes of levels, branching ratios and ionization cross-section; laser parameters such as power, spectral bandwidth, frequency, pulse width (or interaction time) and delay between the pulses; effusive atom source parameters such as atomic velocity distribution and angular divergence (collimation ratio), all have a complex interplay on the ionization efficiency and selectivity of the photoionization process.

The coherent laser–atom interactions can be accurately described by the density matrix theory[19]. The density matrix equations relevant for the pulsed two-step excitation process published in our recent article[8] have been suitably adapted to the cw laser excitation process.

In an AVLIS process, when the first and second excitation lasers are tuned to the frequencies ν_1 and ν_2 respectively, isotope selectivity is defined as

$$\text{Isotope Selectivity S}\ (\nu_1, \nu_2) = \left(\frac{\eta_{176_{Lu}}}{\eta_{175_{Lu}}}\right) \quad (1)$$

Where, η is the ionization efficiency of the isotope

When the abundance of the isotopes is not equal, one needs to normalize the selectivity with the abundance of the constituent isotopes; thus, isotope ratio enhancement factor is defined as

$$\text{Isotope Ratio Enhancement Factor IRE}\ (\nu_1, \nu_2) = \left(\frac{\eta_{176_{Lu}}}{\eta_{175_{Lu}}}\right) * \left(\frac{A_{176_{Lu}}}{A_{175_{Lu}}}\right) \quad (2)$$

Where, A is the fractional abundance of the isotope

Degree of enrichment is calculated using the expression

$$\text{Degree of enrichment}\ (\%) = \left\{\frac{\eta_{176_{Lu}} * A_{176_{Lu}}}{\left(\eta_{175_{Lu}} * A_{175_{Lu}} + \eta_{176_{Lu}} * A_{176_{Lu}}\right)}\right\} * 100 \quad (3)$$

Results and Discussion

For a source temperature of 1600^0 C, the most probable velocity of ^{176}Lu is 421.8 m/s. At this temperature the Doppler broadening of the 465.9316 nm transition is ~ 1500 MHz. Let us consider that the atom source to have a length-to-diameter (L/D) ratio of 5 corresponding to the full-angle divergence (θ) of 22.6^0. For the orthogonal laser-atom interaction, Doppler broadening along the laser propagation axis reduces to ~ 565 MHz. Let us also consider that the laser atom interaction region to have dimensions of 10 mm diameter and 270 mm long.

First, we look at the possibility of using cw lasers for excitation and ionization of ^{176}Lu isotope.

Excitation and ionization using cw lasers

As mentioned earlier, the primary aim of the present work is to investigate the enrichment of ^{176}Lu through off-the-shelf lasers. A detailed survey has been carried out on the availability of laser systems in the wavelength ranges indicated in Table 1. Blue diode laser systems within the wavelength range of the first excitation transition are available with a typical cw power of 30 mW; while diode lasers with accessible wavelengths of the second excitation transition have a typical power of 120 mW. Therefore, we set the limit to the powers of first and second excitation lasers as 30 mW and 120 mW corresponding to the power densities of 38.2 mW/cm^2 and 153 mW/cm^2

respectively. The respective saturation intensities of the transitions 465.9316 nm and 1179.8686 nm 13 mW / cm^2 and 3 mW / cm^2 can be easily achieved using the available cw lasers. The frequency of the excitation lasers can be controlled to ~1 MHz using the commercially available wavelength meters. Non-resonance ionization can be carried out using the high power 10 W cw lasers which are available in wavelengths of 532 nm (Nd:YAG laser) or 527 nm laser (Nd:YVO_4 laser). Therefore, we set the limit to the power of ionization laser to 10 W and corresponding power density is 12.73 W/cm^2.

Calculation of ionization efficiencies of Lu isotopes has been carried out varying the frequencies of the first and second excitation lasers around the resonance of Lu isotopes and the results are plotted as two-dimensional contour plots in Fig. 2. The contours showed resonances in agreement with expected positions (Table 3). Strong diagonal ridges corresponding to the coherent two photoionization have been observed even at longer detunings due to the strong first and second excitation transitions. The resonance frequency position of the most intense hyperfine excitation pathway 17/2-19/2-17/2 (15148.7 MHz, -25159.4 MHz) of ^{176}Lu lies far away from the most intense hyperfine excitation pathway 5-6-5 (11099.0 MHz, -17718.8 MHz) of ^{175}Lu.

Since the most probable velocity of Lu atoms at 1600^0 C is 421.8 m/sec, for the cw laser beam diameter of 1 cm, the interaction time of atoms with spatially overlapped laser beams is 23.7 μs. The cw lasers typically operate in the fundamental mode TEM_{00} having a Gaussian intensity distribution across the diameter; nevertheless it is possible to convert them into a flat-top intensity distribution using beam shaping optics. For the present work, we have considered lasers to have flat-top intensity distribution across its diameter. First, evolution of level populations with interaction time (Fig. 3A and 3B) have been calculated setting the excitation lasers to the frequencies corresponding to the hyperfine excitation pathway of 17/2-19/2-17/2 (15148.7 MHz, -25159.4 MHz) of ^{176}Lu and setting the power of the ionization laser to zero. As expected in the case of non-resonant ^{175}Lu isotope (Fig. 3A), a very small fraction of atoms which are excited into the upper levels decay into the trapped states. At the end of the interaction, about 0.56% atoms can be found in the 1993.92

cm^{-1} trapped level and rest of the atoms in the ground state 0.0 cm^{-1}. On the other hand, for the case of resonant ^{176}Lu isotope (Fig. 3B), the atoms from the ground F = 17/2 hyperfine level are excited through the 17/2-19/2-17/2 hyperfine excitation pathway. Since the ionization laser power is set to zero, the atoms excited into the upper hyperfine levels decay to the 1993.92 cm^{-1}, 4136.13 cm^{-1} and 7476.39 cm^{-1} trapped levels. Due to the repetitive excitation and decay processes, at the end of the interaction, the entire population of F = 17/2 (25%) is transferred to the trapped levels mentioned above. It is therefore expected that the introduction of cw ionization laser transfers atoms from the excited levels into the ionization continuum. The dynamics of the photoionization process with the introduction of a cw ionization laser is discussed below.

When a cw ionization laser with a power density of 12.73 W/cm^2 along with the cw excitation lasers interacts with the atomic beam; the ionization efficiency of the non-resonant ^{175}Lu isotope (Fig. 3C) reaches to the value of 2.3×10^{-10} and the ionization efficiency of resonant ^{176}Lu isotope (Fig. 3D) reaches to 2.5×10^{-5} implying that most of the population excited into the higher levels decays to the trapped states. The low ionization efficiency of the resonant ^{176}Lu isotope can be attributed to multiple factors such as low power density of the cw ionization laser and low ionization cross-section (1×10^{-16} cm^2) of the non-resonant ionization process. From the equations (1)-(3), one can calculate the degree of enrichment, which is ~100%. Considering the Lu number density of 1×10^{13} atoms / cm^3 and the dimensions[7,20] of the laser-atom interaction region of 10 mm diameter and 270 mm length, the production rate of enriched ^{176}Lu is calculated to be 4.9 μg / hour. In comparison to the value of 3.7 mg / hour reported by D'yachkov[17] et al, the production rate in the present case is three orders lower. Therefore, enrichment of ^{176}Lu through *all* cw laser process is very inefficient. Hence, we have adopted a combination of cw lasers for the excitation process and pulsed laser for the ionization process which is discussed in the next section.

cw laser excitation and pulsed laser ionization

As discussed in the previous section, the low ionization efficiency of ^{176}Lu under cw laser excitation and ionization is due to the low non-resonant ionization cross-section and low peak power of the cw

ionization laser. This can be overcome by employing the tunable high repetition rate pulsed laser for the ionization. Modelling of cw laser excitation followed by pulsed laser ionization for the isotope selective photoionization of Sr has been studied previously[21]. Currently high repetition rate (up to 10 KHz) Ti:Sapphire lasers are available with the average power of 1 W. The pulse duration of these lasers is 50 ns. These lasers are also having wavelength tunability between 700 nm – 1000 nm. The lasers can produce peak power density of 2500 W/cm^2. Wavelength tunability of these lasers allows atoms to be excited either into high lying Rydberg states followed by electric field ionization or directly into the autoionization levels. Cross-section[22] for such a process can be in the range of 1×10^{-14} cm^2 which is two-orders higher than the cross-section for the non-resonant ionization process. As a result of high peak power density and the high resonance ionization cross-section, ionization efficiency is expected to be enhanced significantly.

If one carefully observes the time evolution of level populations of the first (21462.38 cm^{-1}) and second (29937.9 cm^{-1}) excited states of ^{176}Lu under cw laser excitation (Fig. 3A and 3B); one can find that the atomic population from these states starts decaying into the trapped states after ~20 ns of its interaction with the excitation lasers. Therefore, for efficient ionization, it is important for the pulsed ionization laser to interact with the *"nascent"* atomic beam within 50 ns of its interaction with the cw lasers. Experimentally, this can be achieved by passing the diode lasers through mechanical choppers and synchronising the pulsed ionization laser with the sync signal of the mechanical chopper.

Evolution of level populations have been calculated for the Lu isotopes by setting the pulsed ionization laser peak power density to 2500 W/cm^2 with a pulse width of 50 ns. The results are plotted in Fig. 4. It can be seen from the Fig. 4B that, in this case the ionization efficiency of ^{176}Lu isotope reaches to the value of 4.7×10^{-2}, in comparison to the ^{175}Lu ionization efficiency of 5.7×10^{-9} (Fig. 4A) corresponding to the degree of enrichment of ~100%. Again, considering the atom number density of 1×10^{13} atoms / cm^3 and the laser-atom interaction region having dimensions of 10 mm diameter and 270 mm length, the production rate of enriched ^{176}Lu is calculated to be 2.7 mg / hour.

This is comparable to the value of 3.7 mg / hour reported by D'yachokov[7] et al. However, in our case the degree of enrichment is significantly higher (100%) than that was previously reported (68.4%).

In the *"nascent"* atomic beam, the population of the ground state 0.0 cm^{-1} is equally distributed among the four hyperfine components F = 11/2 to F = 17/2. Therefore, the F = 17/2 hyperfine level possesses 0.25 (25%) of the population of which 5×10^{-2} is ionized. This implies ionization efficiency of 20% of the targeted F=17/2 hyperfine level population. The ionization efficiency can be further increased by increasing the power of the ionization laser; however, it is not practically viable as tunable high repetition rate lasers with average power > 1 W are not commercially available. Another reason for the low ionization efficiency is due to the large Doppler broadening of the atomic ensemble. As mentioned earlier, for self-collimating atomic beam effusing out of the atom source having L/D ratio of 5 (full angle divergence of 22.6^0), the Doppler broadening along the laser propagation axis will be 565 MHz for the 465.9316 nm transition. The diode laser which can be considered as the single frequency system during short interaction times (50 ns), causes a *"hole burning"* in the velocity groups of the Doppler broadened atomic ensemble. The group of atoms having velocities nearly perpendicular to the laser propagation axis induce a very small proportion of velocity induced Doppler shifts. When the excitation laser is tuned to the resonance of a transition, this group of atoms of the resonant isotope are excited and ionized. The remaining atoms experiencing the velocity induced Doppler shifts are less likely to get excited and ionized. This causes low ionization efficiency. One of the ways to overcome such a problem is by increasing the linewidth of the excitation lasers; however, this is associated with loss in selectivity. Therefore, we have adopted alternative approach. Angular divergence of the atomic beam can be reduced by increasing the L/D ratio of the atom source which causes reduction in the angular divergence and hence velocity induced Doppler shifts. Using this approach, most of the atoms in the atomic beam can be brought into the resonance by adjusting the L/D ratio of the atom source. Calculation of ionization efficiency and degree of enrichment has been carried out varying the L/D ratio of the atom source. It has been found that the L/D ratio 10 corresponding to the full angular divergence 11.5^0 enhances

the ionization efficiency to 8.8×10^{-2} while the degree of enrichment remains at ~100%. Such source geometry allows production of ^{176}Lu at a rate of 5 mg/hour.

Effect of delay of ionization laser

Effect of delay and delay jitter of the ionization laser pulse with reference to the interaction time has been studied. Ionization efficiency and the degree of enrichment have been calculated varying delay of the ionization laser with reference to the start time of interaction of cw excitation lasers with *"nascent"* atomic beam. It has been observed that a delay of 50 ns results in highest ionization efficiency. Therefore, it is necessary to set the delay of the ionization laser to 50ns ± 10 ns to achieve the ionization efficiency within 90% of its value. This requirement can be easily met with the current level of synchronization electronics.

Conclusion

We have proposed a novel and simple method for the enrichment of ^{176}Lu isotope a precursor to ^{177}Lu medical isotope. The physics of the laser-atom interaction has been studied through the dynamics of the atomic level populations using the density matrix formalism. It has been shown that a combination of cw excitation lasers and pulsed ionization laser can be used for the laser isotope separation of ^{176}Lu. The optimum conditions for the efficient and selective separation of ^{176}Lu have been derived by studying the time evolution of level populations during laser excitation. It has been shown that, it is possible to produce ~100% enriched ^{176}Lu isotope at a rate of 5 mg / hour, which is higher than all previously reported methods so far. The enrichment process proposed can be easily adopted using off-the-shelf lasers for similar atomic systems.

References

1) Karl Cohen, Editor: George M Murphy. The Theory of Isotope Separation as Applied to the Large Scale Production of U235. Mcgraw-Hill Book Company Inc., 1951.

2) Jeff W. Eerkens, Jay F. Kunze and Leonard J. Bond. Laser Isotope Enrichment for Medical and Industrial Applications, Proceedings of ICONE14 International Conference on Nuclear Engineering, July 17-20, 2006, Miami, USA.

3) Marion de Jong, Roelf Valkema, Francois Jamar, Larry K.Kvols, Dik J.Kwekkeboom, Wout A.P.Breeman, Willem H.Bakker, Chuck Smith, Stanislas Pauwels and Eric P.Krenning. Somatostatin receptor-targeted radionuclide therapy of tumors: Preclinical and clinical findings. Seminars in Nuclear Medicine, 32, 133-140 (2002).

4) Ashutosh Dash, Maroor Raghavan, Ambikalmajan Pillai and Furn F. Knapp Jr. Production of 177Lu for Targeted Radionuclide Therapy: Available Options. Nucl Med Mol Imaging 49, 85-107 (2015).

5) Zuzana Dvorakova. Production and chemical processing of 177Lu for nuclear medicine at the Munich research reactor FRM-II. Doctoral Thesis, Technische Universiat Munchen, 2007.

6) U. Georg, W. Borchers, M. Keim, A. Klein, P. Lievens, R. Neugart, M. Neuroth, Pushpa M. Rao, Ch. Schulz. Laser spectroscopy investigation of the nuclear moments and radii of lutetium isotopes. Eur. Phys. J. A 3, 225-235 (1998).

7) A.B. D'yachkov, S.K. Kovalevich, A.V. Labozin, V.P. Labozin, S.M. Mironov, V.Ya. Panchenko, V.A. Firsov, G.O. Tsvetkov and G.G. Shatalova. Selective photoionisation of lutetium isotopes. Quantum Electronics 42, 953 – 956 (2012).

8) M. V. Suryanarayana. Isotope selective three-step photoionization of ^{176}Lu. Journal of the Optical Society of America 38B, 353-370 (2021).

9) M.V. Suryanarayana. Isotope separation of ^{176}Lu a precursor to ^{177}Lu medical isotope using broadband lasers. M*anuscript accepted for publication in Scientific Reports*.

10) NIST Atomic Spectra Database, NIST, USA, Weblink: https://physics.nist.gov/PhysRefData/ASD/levels_form.html

11) Atomic spectral line database from CD-ROM 23 of R. L. Kurucz, https://www.cfa.harvard.edu/amp/ampdata/kurucz23/sekur.html.

12) T. Brenner, S. Buttgenbach, W. Rupprecht, and F. Traber. Nuclear moments of the low abundant natural isotope 176Lu and hyperfine anomalies in the lutetium isotopes. Nucl. Phys. A 440, 407–423 (1985).

13) J Vergès and J-F Wyart. Infrared Emission Spectrum of Lutecium and Extended Analysis of Lu I. Phys. Scr. 17, 495 (1978).

14) G. I. Bekov and E. P. Vidolova-Angelova.Optimal scheme for multistage photoionization of lutetium atoms by laser radiation. Sov. J. Quantum Electron. 11(1), 137-139 (1981).

15) V. Gadelshin, T. Cocolios, V. Fedoseev, R. Heinke, T. Kieck, B. Marsh, P. Naubereit, S. Rothe, T. Stora, D. Studer P. Van Duppen and K. Wendt. Laser resonance ionization spectroscopy on lutetium for the MEDICIS project. Hyperfine Interact (2017) 238:28.

16) Vadim Maratovich Gadelshin, Reinhard Heinke, Tom Kieck, Tobias Kron, Pascal Naubereit, Frank Rösch, Thierry Stora, Dominik Studer and Klaus Wendt. Measurement of the laser resonance ionization efficiency for lutetium. Radiochim. Acta 2019; 107(7): 653–661.

17) Ignacio E. Olivares, Andrés E. Duarte, Eduardo A. Saravia, and Francisco J. Duarte. Lithium isotope separation with tunable diode lasers. Applied Optics Vol. 41, 2973-2977 (2002).

18) K Matsuoka, H Niki, I Ogawa, Y Shinki, Y Kawashima and K Matsumura. The laser Isotope separation (LIS) methods for the enrichment of 48Ca. J. Phys.: Conf. Ser. 1468 012199 (2020)

19) B. W. Shore. The Theory of Coherent Atomic Excitation: Simple Atoms and Fields. Vol. 1 (Wiley, 1990).

20) A. P. Babichev, I. S. Grigoriev, A. I. Grigoriev, A. P. Dorovskii, A. B. D'yachkov, S. K. Kovalevich, V. A. Kochetov, V. A. Kuznetsov, V. P. Labozin, A. V. Matrakhov, S. M. Mironov, S. A. Nikulin, A. V. Pesnya, N. I. Timofeev, V. A. Firsov, G. O. Tsvetkov, and G. G. Shatalova. Development of the laser isotope separation method (AVLIS) for obtaining weight amounts of highly enriched 150Nd isotope. Quantum Electron. 35, 879–890 (2005).

21) O. Rhodri Jones, Richard M. Perks, Helmut H. Telle and Tim Grey Morgan. Isotope-specific Resonance Ionization Mass Spectrometry Using Continuous-wave Diode and Pulsed Dye Lasers for Trace Detection and Enrichment of Elements of Environmental and Medical Importance, Exemplified for Strontium (Sr)-Part I: Theoretical Modelling. Rapid Communications in Mass Spectrometry 10, 1725-1738 (1996).

22) A. B. D'yachkov, A. A. Gorkunov, A. V. Labozin, S. M. Mironov, V. Y. Panchenko, V. A. Firsov, and G. O. Tsvetkov. A study of the kinetic parameters of Lu laser photoionization scheme. Opt. Spectrosc. 128, 289–296 (2020).

Data availability: All the relevant data is provided with this paper. Any additional data relevant to the work in this paper are available upon reasonable request to the corresponding author.

Code availability: The code developed is not available for other users.

Author Contributions: MVS conceived the idea and developed the requisite codes. Both the authors contributed towards computations, data interpretation and manuscript preparation.

Competing interests: The authors declare no competing interests.

Additional Information: Correspondence and requests for the additional information should be addressed to the corresponding author.

Acknowledgements: Authors acknowledge the support of Computational Analysis Division, Bhabha Atomic Research Centre, Visakhapatnam for providing the Super Computer Facility for this work.

Table 1. Table of two step photoionization schemes for the laser isotope separation of Lu isotopes.

Ground State	Wavelength of the first excitation laser (nm)	First Excited State	Wavelength of the second excitation laser (nm)	Second Excited State
$5d6s2\ ^2D_{3/2}$ (0.0 cm^{-1})	471.8012	$5s6s6p\ ^4D^0_{3/2}$ (21195.37 cm^{-1})	710.2712	$6s6p^2\ ^4P_{5/2}$ (35274.5 cm^{-1})
			1143.8336	$5d^26s\ ^2P_{3/2}$ (29937.9 cm^{-1})
	465.9316	$5d6s6p\ ^2D^0_{5/2}$ (21462.38 cm^{-1})	1179.8686	$5d^26s\ ^2P_{3/2}$ (29937.9 cm^{-1})
	451.9823	$5d6s6p\ ^2D^0_{3/2}$ (22124.76 cm^{-1})	760.4713	$6s6p^2\ ^4P_{5/2}$ (35274.5 cm^{-1})
			854.2117	$6s6p^2\ ^4P_{3/2}$ (33831.46 cm^{-1})
	411.3857	$5d6s6p\ ^4P^0_{3/2}$ (24308.09cm^{-1})	911.8754	$6s6p^2\ ^4P_{5/2}$ (35274.5 cm^{-1})

Table 2. Table of HFS Coupling Constants of Lutetium energy levels of the 465 nm – 1179 nm photoionization scheme.

Energy Level	^{175}Lu		^{176}Lu		Reference
	A (MHz)	B (MHz)	A (MHz)	B (MHz)	
$5d6s^2\ ^2D_{3/2}$ (0.0 cm^{-1})	194.331617	1511.398650	137.920537	2132.296936	Ref. [12]
$5d6s6p\ ^2D^0_{5/2}$ (21462.38 cm^{-1})	1398.2	-689.5	992.7$^{\#}$ (Computed)	-972.2$^{\$}$ (Computed)	Ref. [13]
$5d^2\ 6s\ ^2P_{3/2}$ (29937.9 cm^{-1})	-1020.8	-1190.2	-724.8$^{\#}$ (Computed)	-1678.2$^{\$}$ (Computed)	

- Calculated from the ratio of A_{176} / A_{175} = 0.71; $ - Calculated from the ratio of B_{176} / B_{175} = 1.41

Table 3. Table of the hyperfine excitation pathways of ^{175}Lu and ^{176}Lu for the 465 nm – 1179 nm photoionization pathway. (The frequency position is with reference to the centre of gravity of ^{176}Lu isotope)

S No	^{175}Lu						^{176}Lu					
	F1-F2-F3	Frequency Position of the first hyperfine transition (MHz)	Normalised Intensity	Frequency Position of the second hyperfine transition (MHz)	Normalised Intensity	Sum two photon frequency position (MHz)	F1-F2-F3	Frequency Position of the first hyperfine transition (MHz)	Normalised Intensity	Frequency Position of the second hyperfine transition (MHz)	Normalised Intensity	Sum two photon frequency position (MHz)
1	2-1-2	-15162.4	23.1	22352.2	23.1	7189.8	11/2-9/2-11/2	-19359.7	50.0	28288.2	50.0	8928.5
2	2-2-2	-12168.9	23.1	19358.7	23.1	7189.8	11/2-11/2-11/2	-13599.9	29.5	22528.4	29.5	8928.5
3	2-2-3	-12168.9	23.1	17146.5	15.4	4977.6	11/2-11/2-13/2	-13599.9	29.5	18836.4	30.5	5236.4
4	3-2-2	-11672.4	15.4	19358.7	23.1	7686.4	13/2-11/2-11/2	-13201.8	30.5	22528.4	29.5	9326.6
5	3-2-3	-11672.4	15.4	17146.5	15.4	5474.1	13/2-11/2-13/2	-13201.8	30.5	18836.4	30.5	5634.5
6	2-3-2	-7752.6	11.5	14942.4	11.5	7189.8	15/2-13/2-11/2	-7290.6	15.6	15846.4	10.5	8555.8
7	2-3-3	-7752.6	11.5	12730.2	33.7	4977.6	15/2-13/2-13/2	-7290.6	15.6	12154.4	43.9	4863.7
8	2-3-4	-7752.6	11.5	8987.1	8.7	1234.4	15/2-13/2-15/2	-7290.6	15.6	6926.1	15.6	-364.5
9	4-3-2	-7601.5	8.7	14942.4	11.5	7340.9	11/2-13/2-11/2	-6918.0	10.5	15846.4	10.5	8928.5
10	4-3-3	-7601.5	8.7	12730.2	33.7	5128.6	11/2-13/2-13/2	-6918.0	10.5	12154.4	43.9	5236.4
11	4-3-4	-7601.5	8.7	8987.1	8.7	1385.5	11/2-13/2-15/2	-6918.0	10.5	6926.1	15.6	8.2
12	3-3-2	-7256.0	33.7	14942.4	11.5	7686.4	13/2-13/2-11/2	-6519.8	43.9	15846.4	10.5	9326.6
13	3-3-3	-7256.0	33.7	12730.2	33.7	5474.1	13/2-13/2-13/2	-6519.8	43.9	12154.4	43.9	5634.5
14	3-3-4	-7256.0	33.7	8987.1	8.7	1731.0	13/2-13/2-15/2	-6519.8	43.9	6926.1	15.6	406.3
15	5-4-3	-3902.3	3.2	6979.7	31.7	3077.4	17/2-15/2-13/2	-2215.9	5.4	4612.7	30.6	2396.8
16	5-4-4	-3902.3	3.2	3236.5	34.3	-665.7	17/2-15/2-15/2	-2215.9	5.4	-615.6	44.0	-2831.4
17	5-4-5	-3902.3	3.2	-2717.5	3.2	-6619.8	17/2-15/2-17/2	-2215.9	5.4	-7794.9	5.4	-10010.8
18	4-4-3	-1851.0	34.3	6979.7	31.7	5128.6	15/2-15/2-13/2	251.1	44.0	4612.7	30.6	4863.7
19	4-4-4	-1851.0	34.3	3236.5	34.3	1385.5	15/2-15/2-15/2	251.1	44.0	-615.6	44.0	-364.5
20	4-4-5	-1851.0	34.3	-2717.5	3.2	-4568.6	15/2-15/2-17/2	251.1	44.0	-7794.9	5.4	-7543.8
21	3-4-3	-1505.5	31.7	6979.7	31.7	5474.1	13/2-15/2-13/2	1021.9	30.6	4612.7	30.6	5634.5
22	3-4-4	-1505.5	31.7	3236.5	34.3	1731.0	13/2-15/2-15/2	1021.9	30.6	-615.6	44.0	406.3
23	3-4-5	-1505.5	31.7	-2717.5	3.2	-4223.1	13/2-15/2-17/2	1021.9	30.6	-7794.9	5.4	-6773.0
24	5-5-4	3064.3	23.7	-3730.0	60.9	-665.7	17/2-17/2-15/2	6113.5	29.6	-8944.9	60.4	-2831.4
25	5-5-5	3064.3	23.7	-9684.1	23.7	-6619.8	17/2-17/2-17/2	6113.5	29.6	-16124.2	29.6	-10010.8
26	4-5-4	5115.5	60.9	-3730.0	60.9	1385.5	15/2-17/2-15/2	8580.4	60.4	-8944.9	60.4	-364.5
27	4-5-5	5115.5	60.9	-9684.1	23.7	-4568.6	15/2-17/2-17/2	8580.4	60.4	-16124.2	29.6	-7543.8
28	5-6-5	11099.0	100.0	-17718.8	100.0	-6619.8	17/2-19/2-17/2	15148.7	100.0	-25159.4	100.0	-10010.8

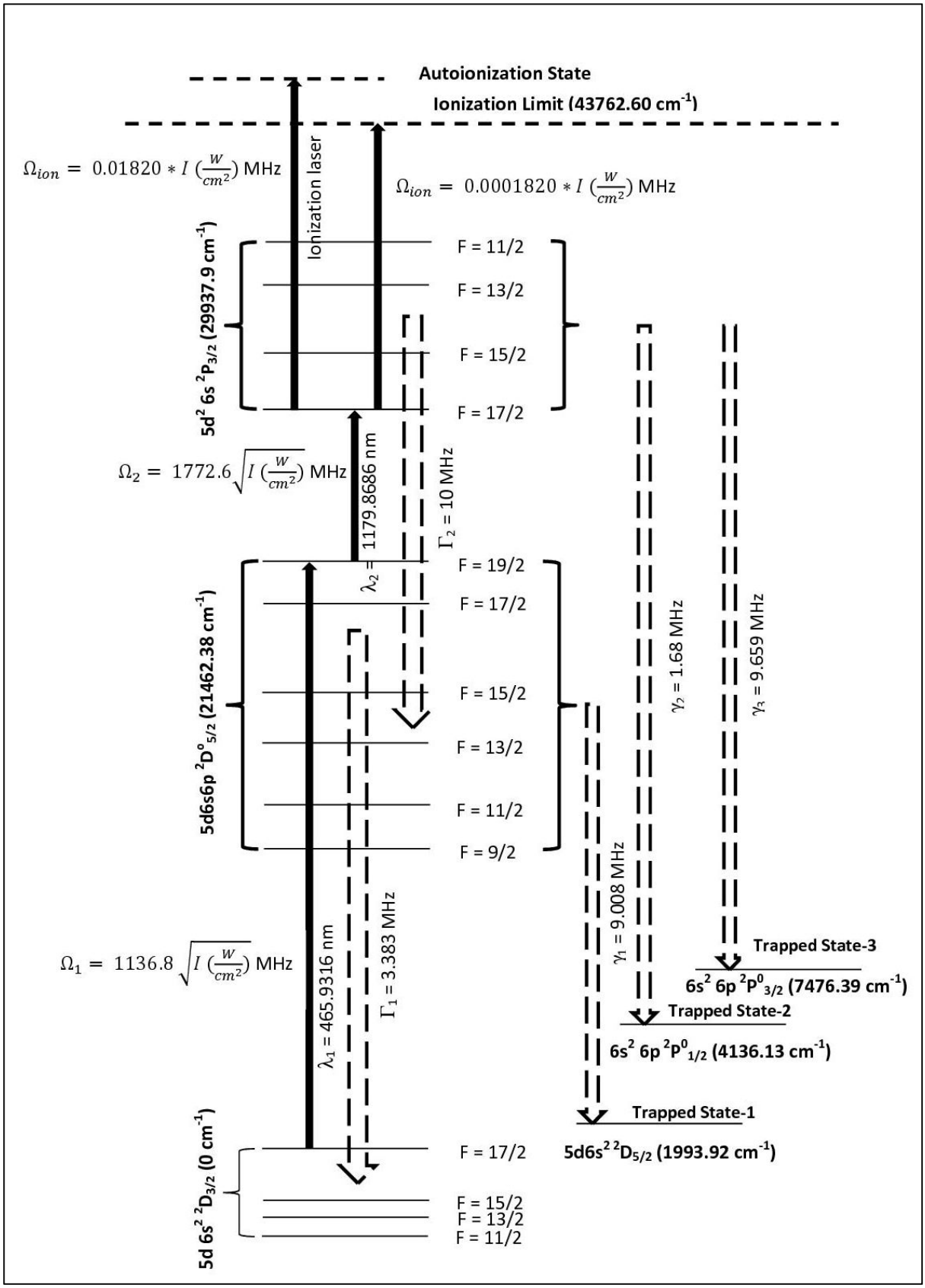

Figure 1. Schematic of the photoionization pathway of ^{176}Lu (not to the scale). The excitation rate (Rabi frequency), decay rate to lower level and decay rate to trapped levels are represented by Ω, Γ and γ respectively.

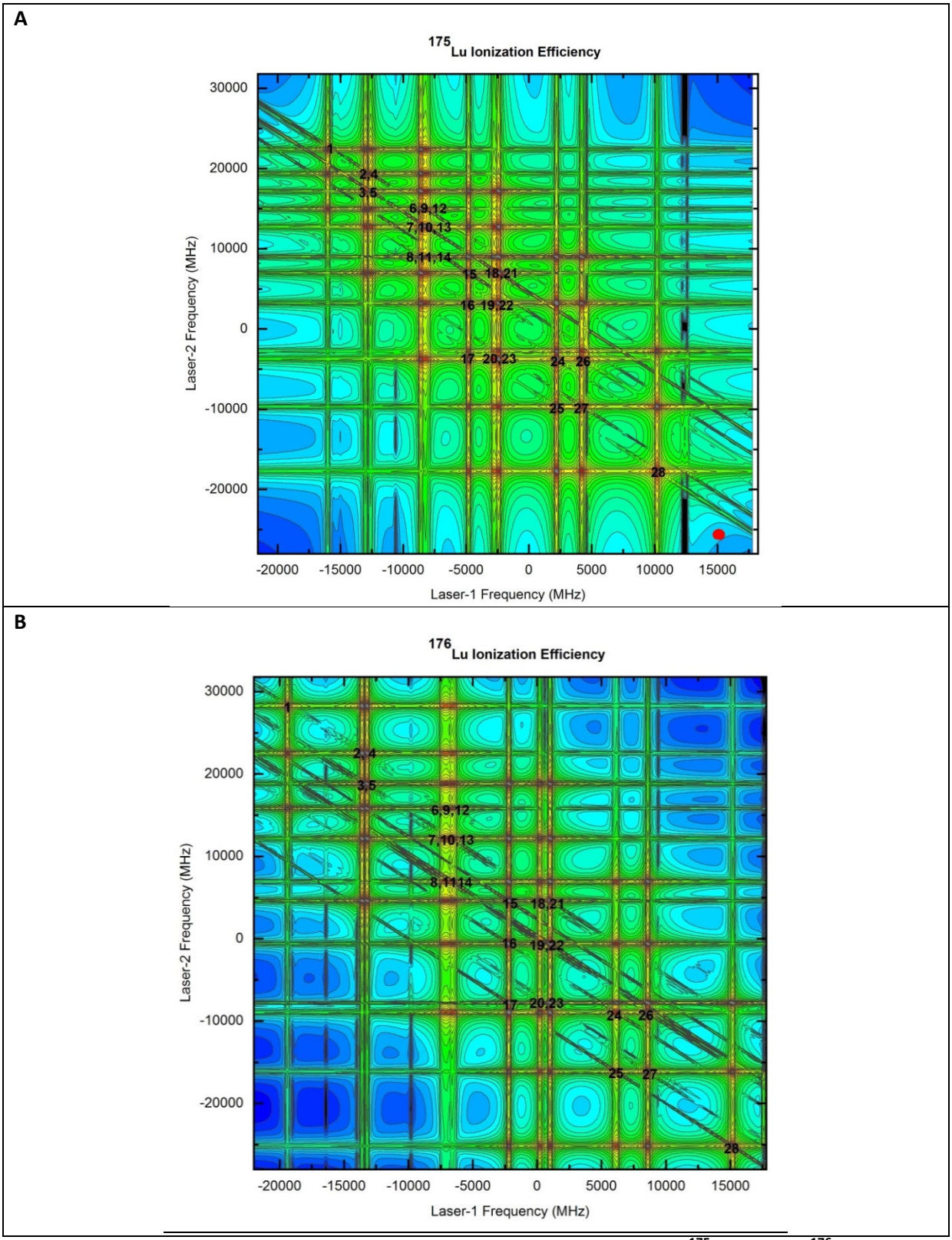

Figure 2. Two dimensional contour plots of ionization efficiencies of (A) ^{175}Lu and (B) ^{176}Lu isotopes under Doppler free conditions. The excitation and ionization laser power densities are 0.038 W/cm2, 0.153 W/cm2 and 12.73 W/cm2 respectively. Full angle divergence of the atomic beam is 22.6^0 and both excitation lasers are counter propagating having frequency jitter of 1 MHz. Resonance frequency positions of the hyperfine excitation pathways have been numbered as per Table 3. Resonance frequency position of 17/2-19/2-17/2 (15148.7 MHz, -25159.4 MHz) of ^{176}Lu isotope is shown as red circle in Fig. 2A.

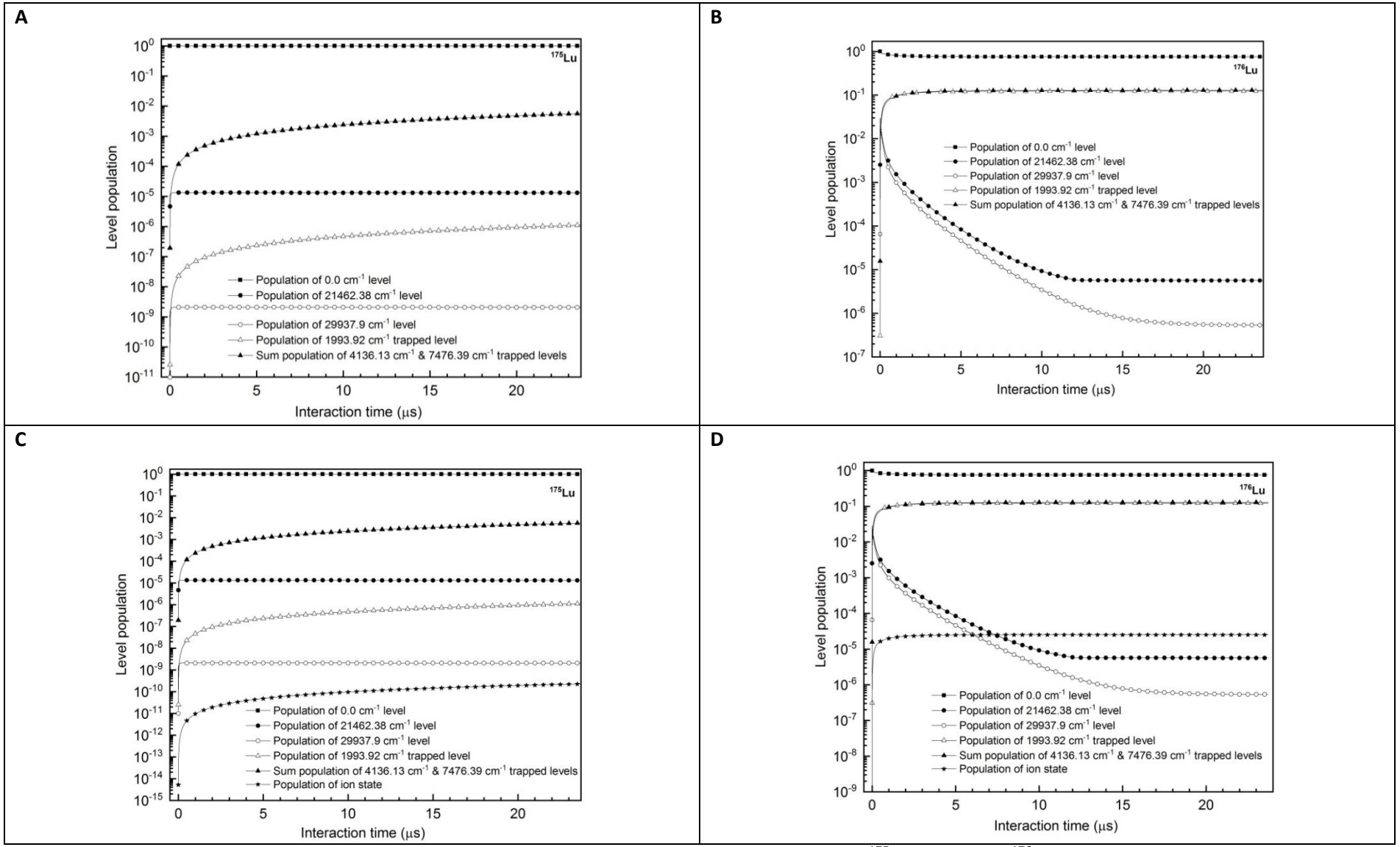

Figure 3 Time evolution of level populations of the ground, excited, ion and trapped states of ^{175}Lu (A, C) and ^{176}Lu (B, D) under cw laser excitation. For graphs (A) and (B) excitation and ionization laser power densities are 0.038 W/cm^2, 0.153 W/cm^2 and 0.0 W/cm^2 respectively. For graphs (C) and (D) excitation and ionization laser power densities are 0.038 W/cm^2, 0.153 W/cm^2 and 12.73 W/cm^2 respectively. Full angle divergence of the atomic beam is 22.6^0 and both excitation lasers are counter propagating having frequency jitter of 1 MHz. Excitation lasers are set to the frequencies corresponding to the hyperfine excitation pathway 17/2-19/2-17/2 (15148.7 MHz, -25159.4 MHz) of ^{176}Lu isotope.

A

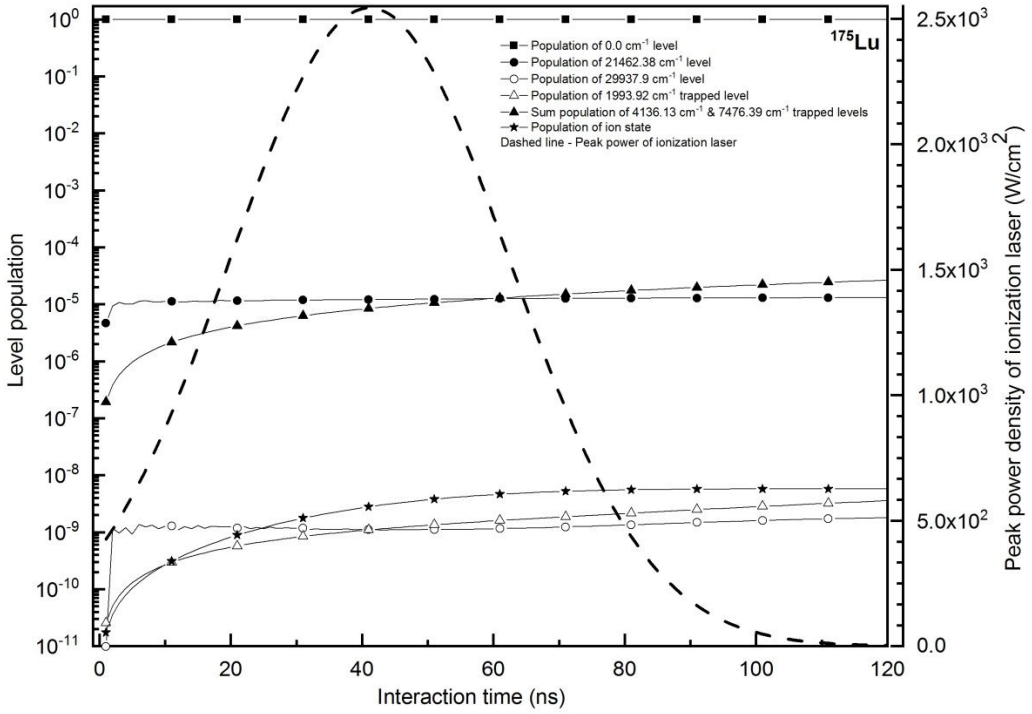

B

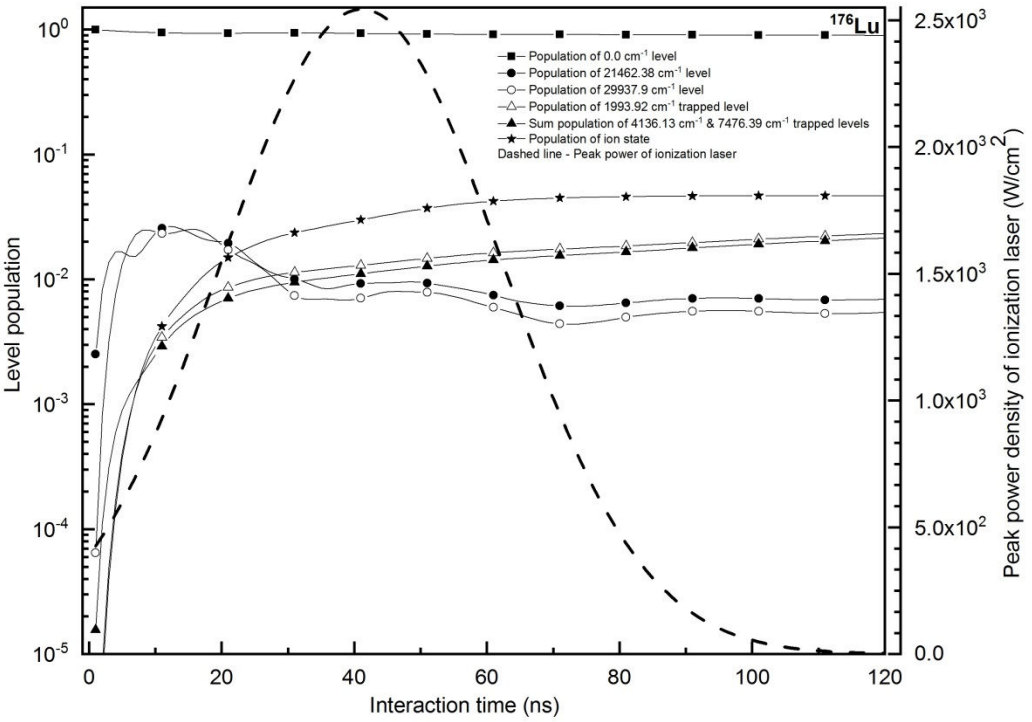

Figure 4. Time evolution of level populations of the ground, excited, ion and trapped states of (A) ^{175}Lu and (B) ^{176}Lu under cw laser excitation and pulsed laser ionization. Excitation laser power densities are 0.038 W/cm^2, 0.153 W/cm^2 respectively and frequency jitter of excitation lasers is 1 MHz. Peak power density of the ionization laser is 2500 W/cm^2 with a pulsed width of 50 ns. Full angle divergence of the atomic beam is 22.6^0 and both excitation lasers are counter propagating. Excitation lasers are set to the frequencies corresponding to the hyperfine excitation pathway 17/2-19/2-17/2 (15148.7 MHz, -25159.4 MHz) of ^{176}Lu isotope.

Figures

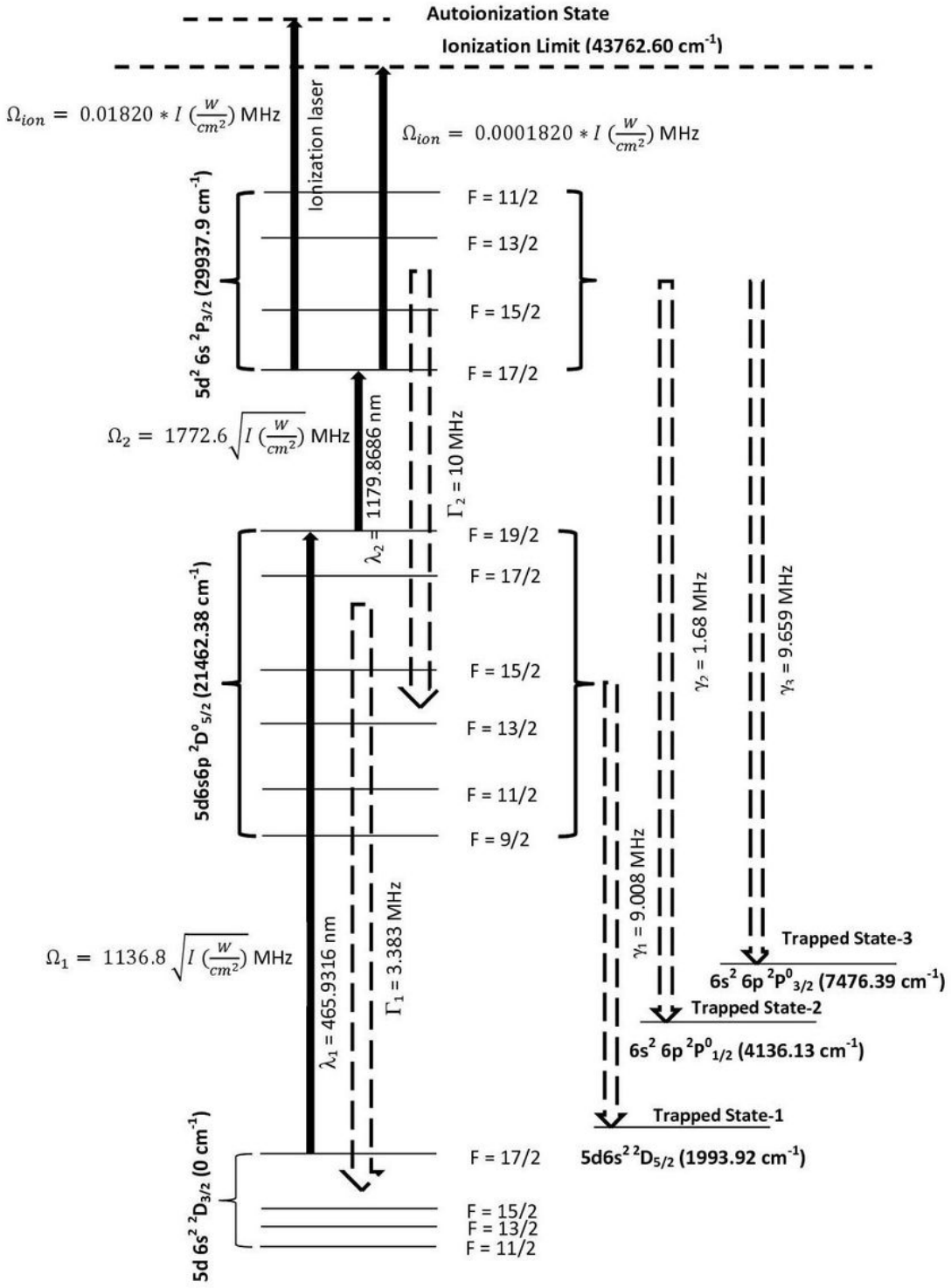

Figure 1

Schematic of the photionization pathway of 176Lu (not to the scale). The excitation rate (Rabi frequency), decay rate to lower level and decay rate to trapped levels are represented by n, Γ and γ respectively.

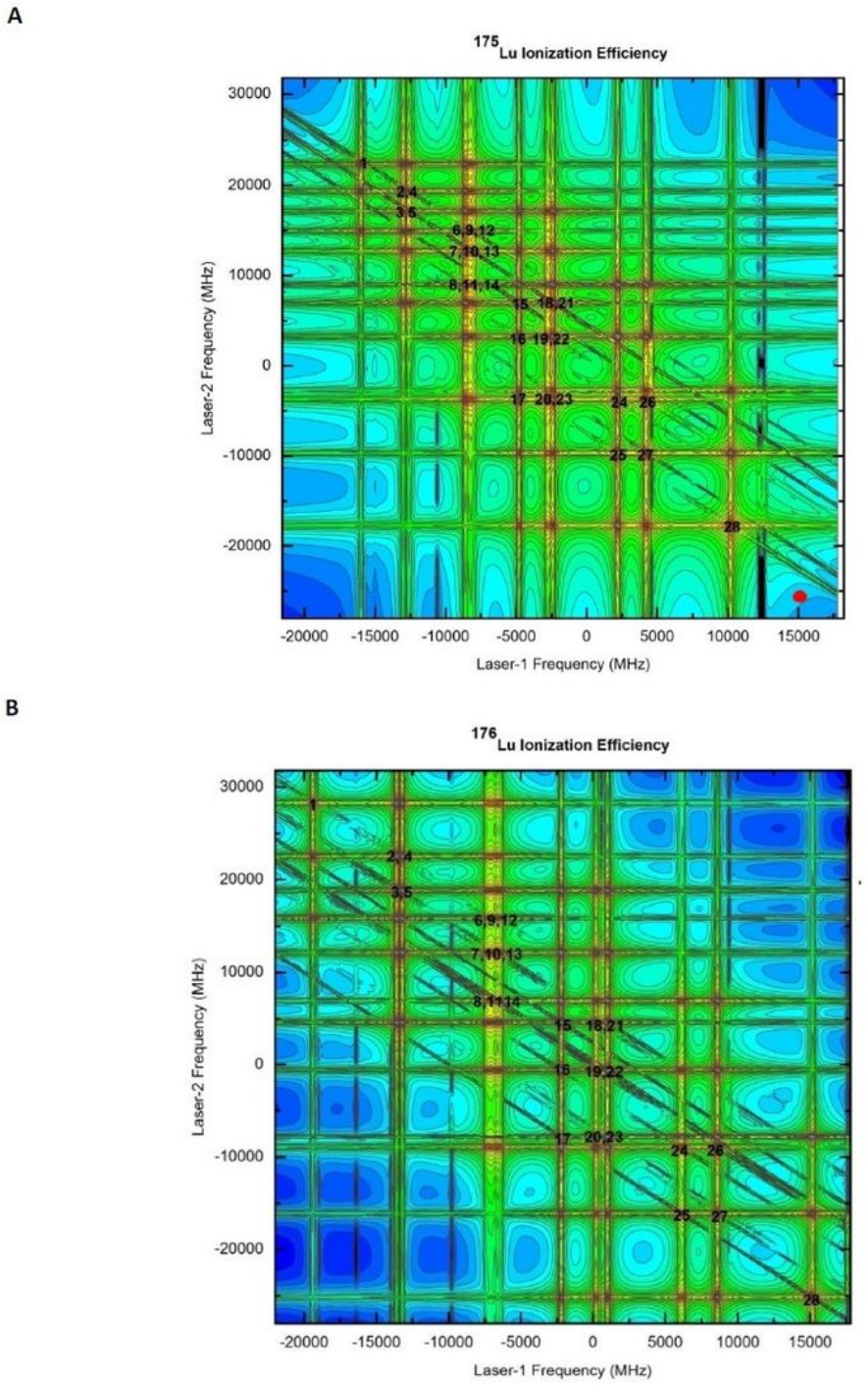

Figure 2

Two dimensional contour plots of ionization efficiencies of (A) 175Lu and (B) 176Lu isotopes under Doppler free conditions. The excitation and ionization laser power densities are 0.038 W/cm2, 0.153 W/cm2 and 12.73 W/cm2 respectively. Full angle divergence of the atomic beam is 22.60 and both excitation lasers are counter propagating having frequency jitter of 1 MHz. Resonance frequency positions of the hyperfine excitation pathways have been numbered as per Table 3. Resonance frequency

position of 17/2-19/2-17/2 (15148.7 MHz, -25159.4 MHz) of 176Lu isotope is shown as red circle in Fig. 2A.

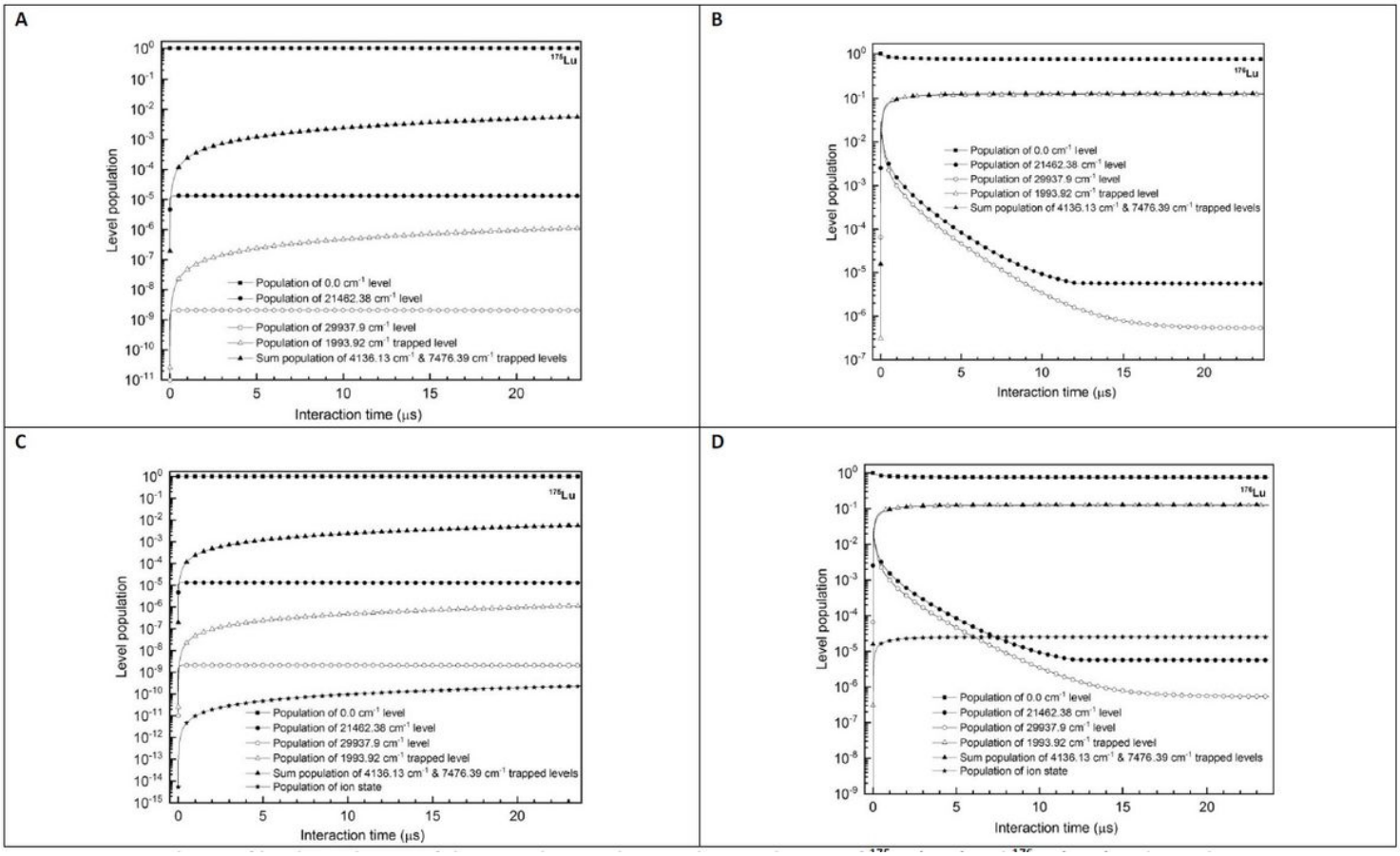

Figure 3

Time evolution of level populations of the ground, excited, ion and trapped states of 175Lu (A, C) and 176Lu (B, D) under cw laser excitation. For graphs (A) and (B) excitation and ionization laser power densities are 0.038 W/cm2, 0.153 W/cm2 and 0.0 W/cm2 respectively. For graphs (C) and (D) excitation and ionization laser power densities are 0.038 W/cm2, 0.153 W/cm2 and 12.73 W/cm2 respectively. Full angle divergence of the atomic beam is 22.60 and both excitation lasers are counter propagating having frequency jitter of 1 MHz. Excitation lasers are set to the frequencies corresponding to the hyperfine excitation pathway 17/2-19/2-17/2 (15148.7 MHz, -25159.4 MHz) of 176Lu isotope.

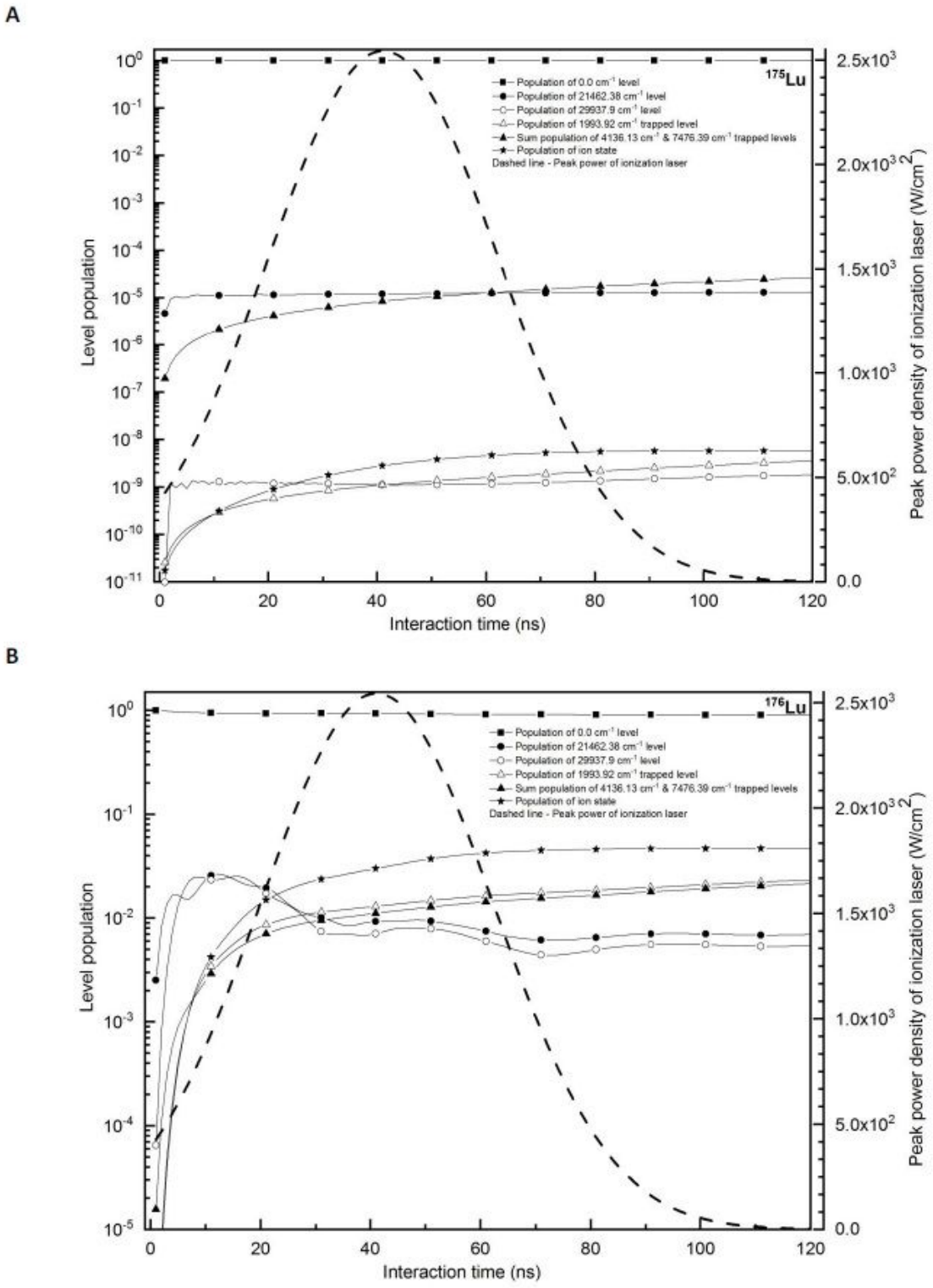

Figure 4

Time evolution of level populations of the ground, excited, ion and trapped states of (A) 175Lu and (B) 176Lu under cw laser excitation and pulsed laser ionization. Excitation laser power densities are 0.038 W/cm2, 0.153 W/cm2 respectively and frequency jitter of excitation lasers is 1 MHz. Peak power density of the ionization laser is 2500 W/cm2 with a pulsed width of 50 ns. Full angle divergence of the atomic beam is 22.60 and both excitation lasers are counter propagating. Excitation lasers are set to the

frequencies corresponding to the hyperfine excitation pathway 17/2- 19/2-17/2 (15148.7 MHz, -25159.4 MHz) of 176Lu isotope.

Supplementary Files

This is a list of supplementary files associated with this preprint. Click to download.

- Supplementarymaterial.pdf